Zangani et al., http://www.jem.org/cgi/content/full/jem.20061220/DC1

SUPPLEMENTAL MATERIALS AND METHODS

Microarray CGH

High molecular weight DNA was purified from lymphomatous or control spleen sections frozen in OCT, with DNeasy tissue kit from QIAGEN, according to the manufacturer's protocol. DNA integrity was assessed by EtBr-stained agarose gel electrophoresis and concentration was measured using a fluorometer. As a control, splenic tissue DNA was prepared from male and female Id^+ mice. Mouse genome CGH microarray 244a (Agilent Technologies) containing 244,000 in situ synthesized oligonucleotide probes was used for comparative genomic hybridization. Approximately 1.5 μg of total genomic DNA (lymphoma and control) was digested, labeled, and hybridized according to the supplier's instructions. The arrays were scanned using a G2565BA scanner (Agilent technologies). Grayscale images were analyzed using Feature Extraction Software v9.1 (Agilent technologies), spots were automatically segmented, and foreground and background intensities were calculated for each spot. Further data processing, normalization, and analysis were performed in CGH analytics v3.4 (Agilent technologies), a software specifically designed for the analysis of Agilent microarrays. To determine DNA copy number changes, a z score algorithm with a threshold of two and a minimum of three consecutive probes was used.

Lymphomas subjected to CGH analysis were as follows: (a) lymphomas generated with eight Th2 cell transfers into Id^+ mice (C2–4, X, Y, and C4–6). (b) Lymphomas generated with two Th2 cell transfers into an Id^+ mouse (Lx2P). (c) Lymphomas from part a that were transferred into a first recipient and killed after 6 wk (C4–2S, X_{R1}, Y_{R1}, and C4–6S). Lymphoma lines X and Y correspond to the lines that were sequenced for V_H expression (Figs. S7–S10).

Southern analysis

High molecular weight DNA from sections or from liver cells were prepared (see previous section). Southern analysis was performed with a J_H probe, a 0.8-kb EcoRI fragment containing part of JH-Cμ intron (6). The probe was labeled with ^{32}P using the Rediprime II random prime labeling system (GE Healthcare). The GeneRuler DNA ladder mix was purchased from Fermentas. Electrophoresis of 5 μg DNA was performed in 0.8% agarose gels and gels were denatured, neutralized, and transferred onto nylon membranes (Millipore) using a vacuum blotter (Qbiogene). Membranes were dried, cross-linked, and hybridized with the labeled probe overnight, using standard procedures with ExpressHyb (CLONTECH Laboratories, Inc.). Images were generated using ImageQuant software (GE Healthcare) after scanning on a Typhoon 9410 phosphoimager (GE Healthcare).

REFERENCES

1. Pillai, S., A. Cariappa, and S.T. Moran. 2005. Marginal zone B cells. *Annu. Rev. Immunol.* 23:161–196.

2. Phan, T.G., S. Gardam, A. Basten, and R. Brink. 2005. Altered migration, recruitment, and somatic hypermutation in the early response of marginal zone B cells to T cell-dependent antigen. *J. Immunol.* 174:4567–4578.

3. Strausberg, R.L., E.A. Feingold, L.H. Grouse, J.G. Derge, R.D. Klausner, F.S. Collins, L. Wagner, C.M. Shenmen, G.D. Schuler, S.F. Altschul, et al. 2002. Generation and initial analysis of more than 15,000 full-length human and mouse cDNA sequences. *Proc. Natl. Acad. Sci. USA.* 99:16899–16903.

4. Haines, B.B., C.V. Angeles, A.P. Parmelee, P.A. McLean, and P.H. Brodeur. 2001. Germline diversity of the expressed BALB/c VhJ558 gene family. *Mol. Immunol.* 38:9–18.

5. Kasturi, K.N., R. Mayer, C.A. Bona, V.E. Scott, and C.L. Sidman. 1990. Germline V genes encode viable motheaten mouse autoantibodies against thymocytes and red blood cells. *J. Immunol.* 145:2304–2311.

6. Pelanda, R., S. Schwers, E. Sonoda, R.M. Torres, D. Nemazee, and K. Rajewsky. 1997. Receptor editing in a transgenic mouse model: site, efficiency, and role in B cell tolerance and antibody diversification. *Immunity.* 7:765–775.

7. Bogen, B., and S. Weiss. 1991. A rearranged lambda 2 light gene chain retards but does not exclude kappa and lambda 1 expression. *Eur. J. Immunol.* 21:2391–2395.

8. Wu, G.E., N. Govindji, N. Hozumi, and H. Murialdo. 1982. Nucleotide sequence of a chromosomal rearranged lambda 2 immunoglobulin gene of mouse. *Nucleic Acids Res.* 10:3831–3843.

9. Banerji, J., L. Olson, and W. Schaffner. 1983. A lymphocyte-specific cellular enhancer is located downstream of the joining region in immunoglobulin heavy chain genes. *Cell.* 33:729–740.

10. Gillies, S.D., S.L. Morrison, V.T. Oi, and S. Tonegawa. 1983. A tissue-specific transcription enhancer element is located in the major intron of a rearranged immunoglobulin heavy chain gene. *Cell.* 33:717–728.

www.jem.org/cgi/doi/10.1084/jem.20061220

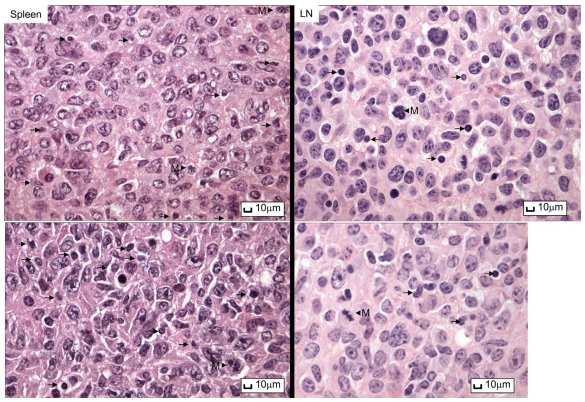

Figure S1. Large cell lymphoma with high magnification. Typical examples of lymphoma histology from different mice. Left, spleen; right, lymph node. Some of the infiltrating smaller, dense lymphocytes are indicated with arrows. Some of the mitotic figures (M) are indicated (arrowheads).

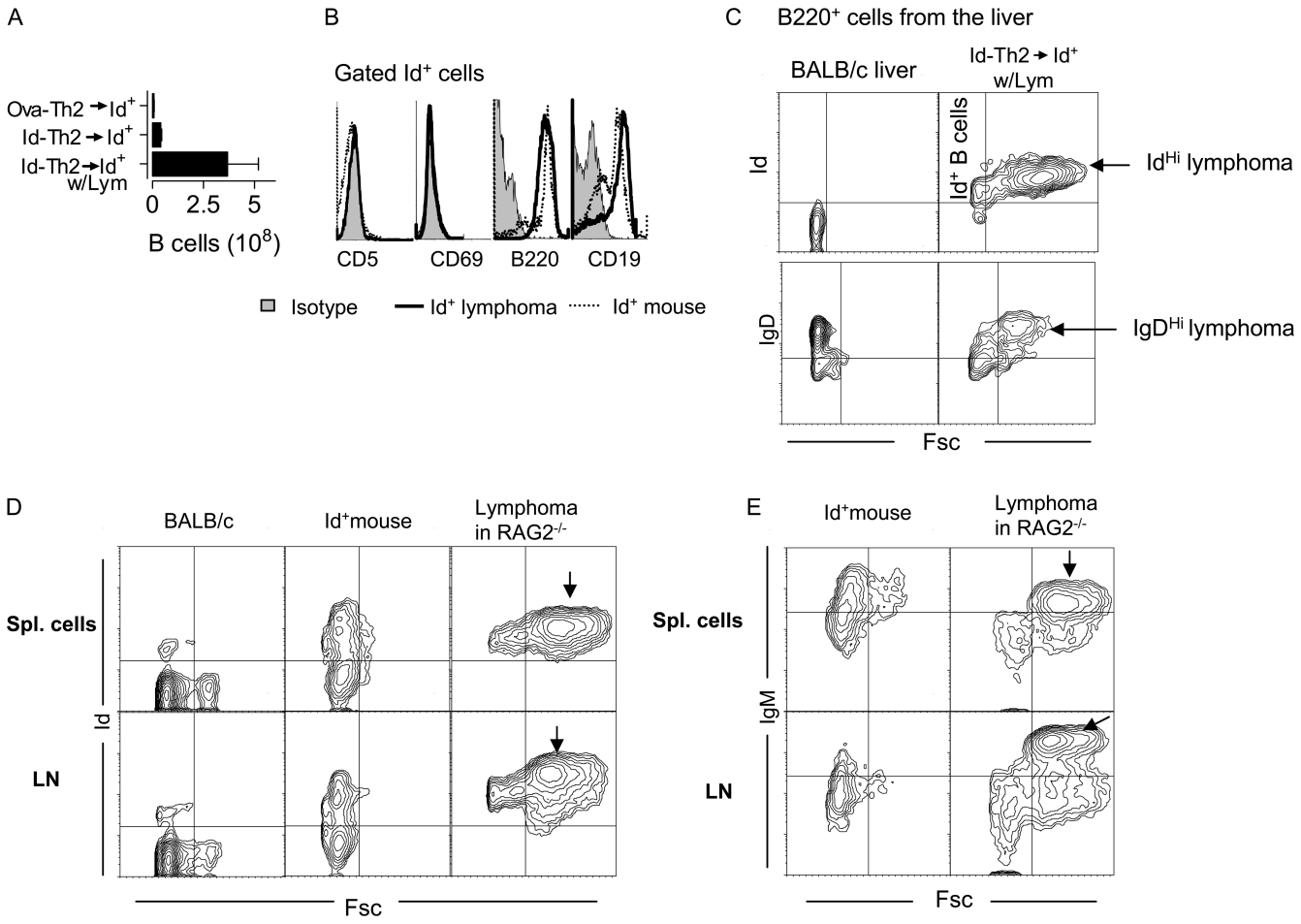

Figure S2. Additional phenotype characterization of lymphoma cells. (A and B) Spleens from the indicated mice were counted and stained 200 d after completion of T cell injections. (A) Splenic B cell numbers in Ova-Th2→Id$^+$ mice compared with Id-Th2→Id$^+$ without and with tumors (w/Lym). (B) Flow cytometric phenotype of induced splenic lymphoma cells. The intensity of staining in lymphoma-bearing mice was compared with healthy Id$^+$ control mice and isotype control. Gated Id$^+$ cells were analyzed for the indicated markers, compared with isotype controls. (C) Gated B220$^+$ B cells in the liver of Id-Th2→Id$^+$ mouse with lymphoma (control: BALB/c mouse). (top) Id versus Forward scatter (Fsc). (right) Id^{Hi} lymphoma are blasts with high Fsc (arrow). In the same mouse is found Id$^+$ B cells with low Fsc suggestive of small nontransformed lymphocytes (top left). (bottom) IgD versus Fsc in another mouse with lymphoma, showing IgD^{Hi} lymphoma blasts (top right), as well as putatively normal IgD$^-$ B cells (bottom left). (D and E) To remove normal B cells from the analysis, lymphoma cells were transferred into recipients. RAG2$^{-/-}$ recipients were analyzed after clinical symptoms appeared, 6–8 wk after transfer. BALB/c and Id$^+$ mice serve as controls (D) Gated B220$^+$ spleen (top) and lymph node (bottom) cells are large Id^{HI} lymphoma cells (arrows). (E) Gated B220$^+$ spleen (top) and LN cells (bottom) are IgM^{Hi} blasts (arrows).

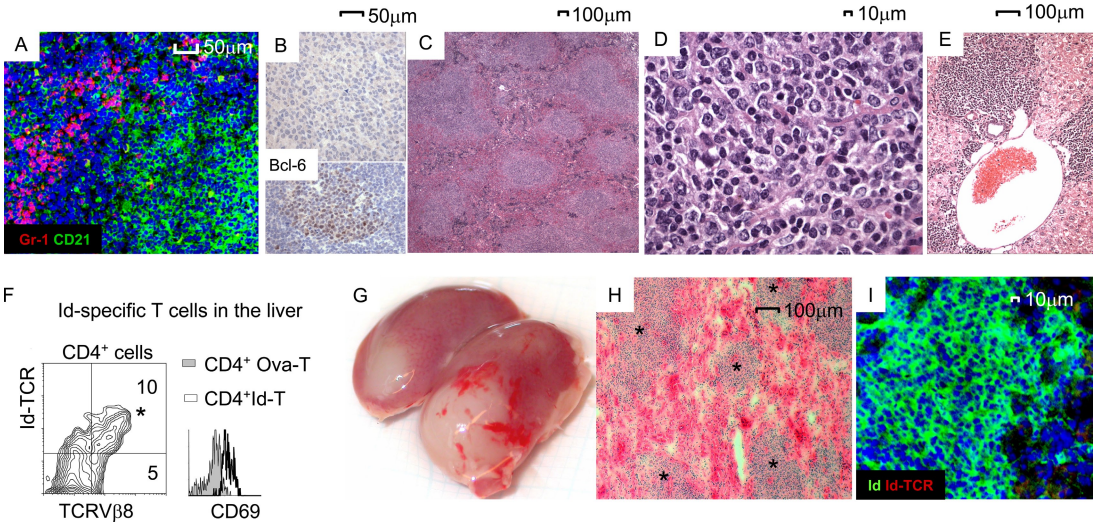

Figure S3. Additional information on lymphoma cells in sections and T cells in the liver and kidney. (A) CD21 (green) versus Gr-1 (Ly-6G, RB6-875 mAb; red). $CD21^+$ lymphoma cells are situated in the white pulp, surrounded by $Gr\text{-}1^+$ granulocytes in the red pulp. (B) Absence of BCL-6 staining in large cell lymphoma (top) compared with control Id^+ spleen (bottom) that shows nuclear staining of BCL-6 in normal germinal center B cells. (C) A minority of the mice (≈10–15%) had nodular lymphoproliferations in their spleens, a finding that may reflect ongoing (polyclonal) Id-driven T–B collaboration or a variant form of the lymphoma. Low power magnification (hematoxylin and eosin) is shown. (D) High power magnification of nodular form (hematoxylin and eosin) showing large cells interspersed with normal dense lymphoid cells. (E) Periportal infiltrates of lymphoma cells (see also Fig. 2, B and D). (F) T cells in liver with lymphoma. (left) Gated $CD4^+$ cells in contour plot. Id-TCR (detected by clonotype-specific mAb GB113) versus TCRVβ8 (F23.1 mAb, which detects the transgenic TCR β chain). Id-specific T cells (Id-T) are identified with an asterisk. (right) CD69 expression of gated Id-specific T cells ($CD4^+F23.1^+GB113^+$, open curve) in the liver of Id-Th2→Id^+ mouse with lymphoma. As a control, the CD69 expression of Ova-T cells (Ova-T, $CD4^+F23.1^+GB113^-$; filled histogram) in the liver of a Ova-Th2–injected Id^+mouse is shown. (G) Photo of kidneys with whitish areas of lymphoma infiltration. (H and I) Kidney sections from mice with lymphoma. (H) Low-power magnification (hematoxylin and eosin) of kidney. Multiple lymphoma infiltrates are indicated (*). (I) Immunohistochemistry of kidney lymphoma. Id (green) versus Id-specific TCR (red). Only Id^+ lymphoma and no red Id-specific T cells are seen.

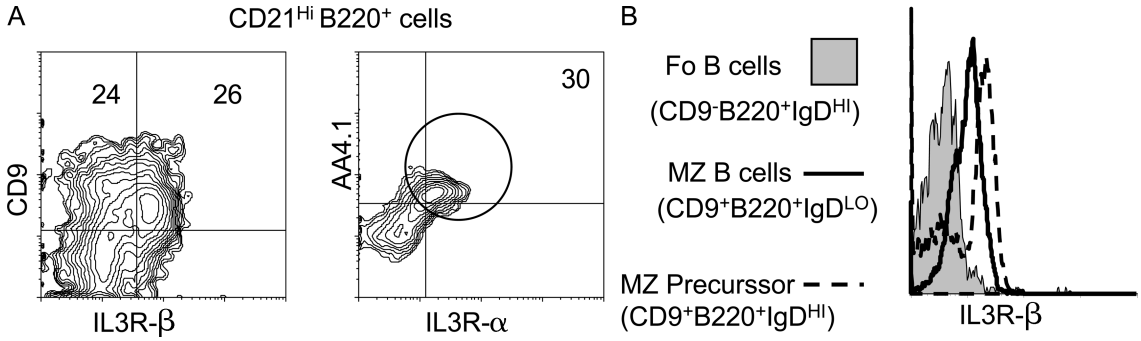

Figure S4. Expression of the IL-3 receptor on splenic B cells. BALB/c spleens were stained for marginal zone markers. (A) $CD21^{HI}B220^+$ cells are shown. (left) The marginal zone B cell marker CD9 (1) is coexpressed with IL3R-Beta (top right quadrant). (right) AA4.1, a marker found on recent bone marrow B cell emigrants and marginal zone B cell precursors, is coexpressed with IL3R-α (circle). (B) IL3R-β expression on splenic B cells. Populations (Fo B cells, MZ B cells, and MZ precursors) are gated as indicated.

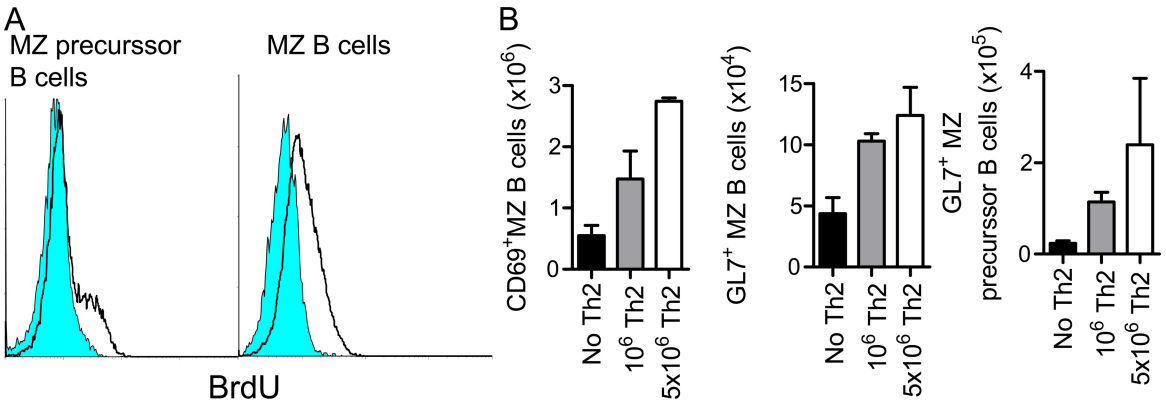

Figure S5. Injected Id-specific Th2 cells induce activation and proliferation of splenic marginal zone precursor B cells in Id$^+$ mice. Id-specific Th2 cells were injected into Id$^+$ mice ($n = 4$), three uninjected Id$^+$ mice served as controls. Mice received a BrdU injection (1 mg i.p.) on day 4. Splenocytes were isolated on day 6 and stained. (A) BrdU incorporation in gated marginal zone precursor B cells (left; CD9$^+$AA4.1$^+$B220$^+$) and marginal zone B cells (right; CD9$^+$CD23$^-$B220$^+$). (B) Total numbers of activated cells of the marginal zone B cell lineage in the spleens. Left, CD69$^+$ marginal zone B cells (Id$^+$CD9$^+$B220$^+$); middle, GL7$^+$ marginal zone B cells (CD9$^+$B220$^+$CD23$^-$); right, marginal zone precursor B cells (CD9$^+$B220$^+$CD23$^{+/Lo}$). GL7 is an activation marker associated with both germinal center B cells and activated marginal zone B cells (2).

Figure S6. Lymphoma-like B cells and Id-specific T cells are detected in the blood before clinical signs. (A–C) Six Id$^+$ mice were injected with 8× Id-specific Th2 cells as described in Fig. 1. Blood was drawn 10 d after each T cell injection (not depicted), and thereafter intermittently in the latency phase. Three of these six mice eventually developed lymphoma. Three examples are shown (from left to right): an Id$^+$ noninjected control mouse, a Th2-injected Id$^+$ mouse that developed lymphoma, and a Th2-injected mouse that did not develop lymphoma. (A) Staining of blood lymphocytes (Fsc-Ssc gate) 15 d after the final Th2 cell injection, corresponding to 215 d before detection of lymphoma. Gated CD19$^+$B220$^+$ cells. Id versus forward scatter (Fsc). (B and C) Staining of blood lymphocytes 115 d after final Th2 cell injection (115 d before lymphoma). (B, top and middle row) Gated CD19$^+$B220$^+$ cells were analyzed for Id versus Fsc and IgM versus Fsc. (arrows) Id^{Hi}/IgM^{Hi} blasts, corresponding to lymphoma cells as shown in Fig. 3 (B and G) and Fig. S2 (D and E). (bottom row) Gated CD4$^+$ cells were analyzed for Id-specific TCR (detected by the GB113 mAb) versus Fsc. The arrow indicates presence of Id-specific CD4$^+$ T cell blasts in a mouse that eventually develop B cell lymphoma. (C) Linear regression analysis of percentage IgM^{Hi} blasts versus Id-specific (GB113$^+$) CD4$^+$ T cell blasts (data from B, 115 d before lymphoma). All six Id$^+$ mice injected with Id-specific Th2 cells are shown. The three mice that later developed lymphoma are marked with asterisks.

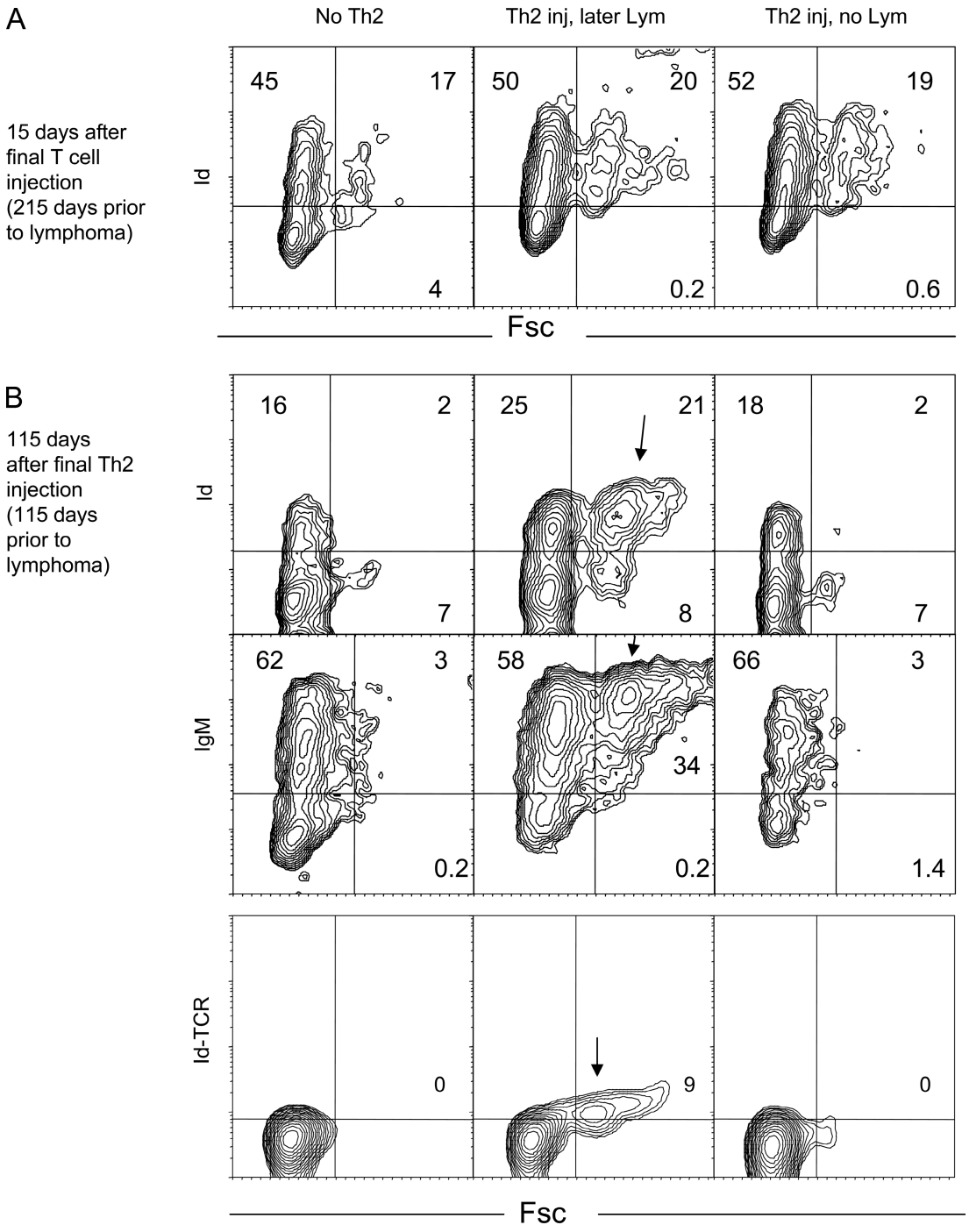
A
No Th2
Th2 inj, later Lym
Th2 inj, no Lym
15 days after final T cell injection (215 days prior to lymphoma)
Id
45
17
4
50
20
0.2
52
19
0.6
Fsc
B
115 days after final Th2 injection (115 days prior to lymphoma)
Id
16
2
7
25
21
8
18
2
7
IgM
62
3
0.2
58
34
0.2
66
3
1.4
Id-TCR
0
9
0
Fsc
C
P< 0.0001
r2=0.9992
IgMHi blasts
Id-spec T cells

Figure S6.

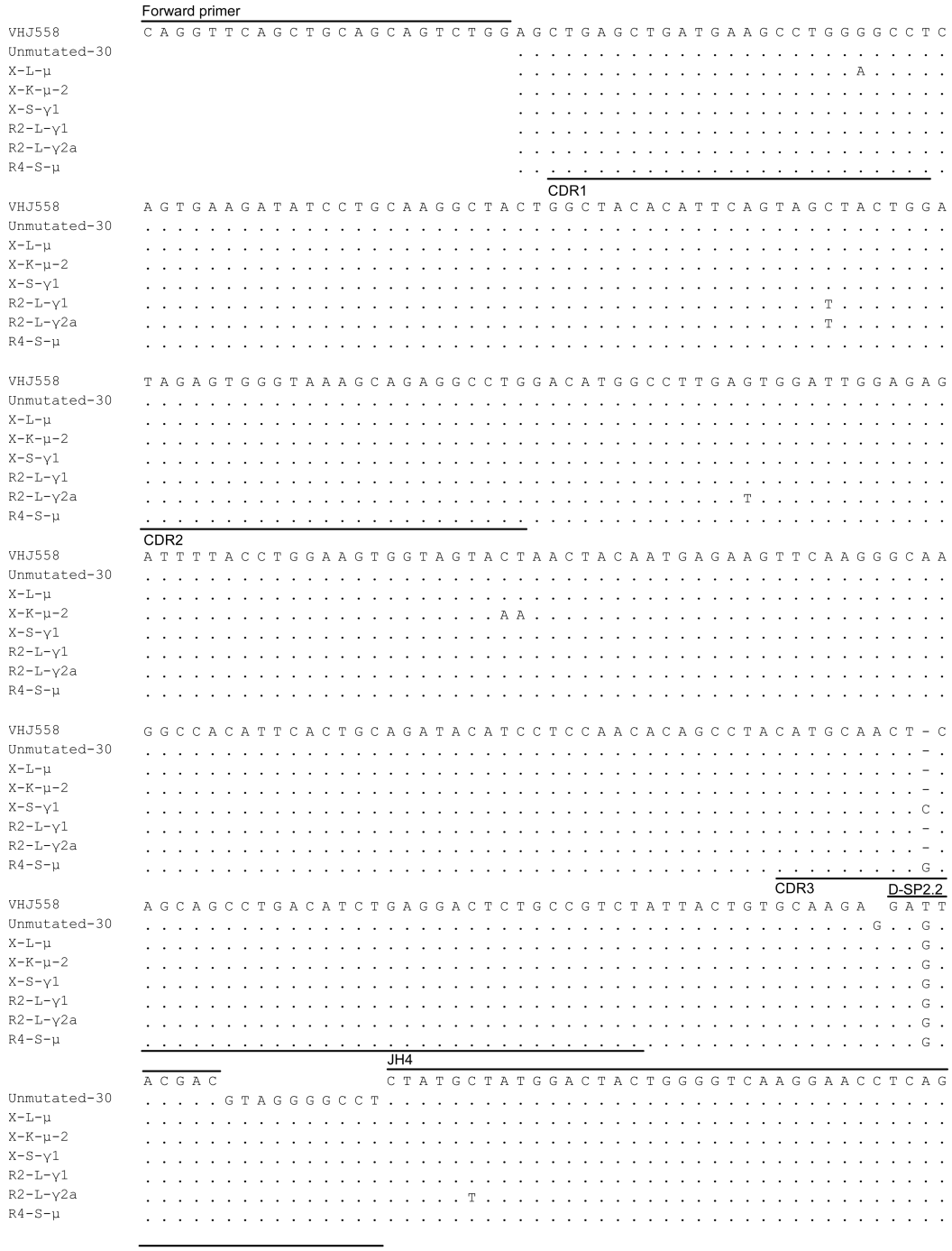

Figure S7. Sequences found in mouse X and its recipients. Altogether, 38 rearranged VDJ sequences were obtained from lymphomatous spleens, livers, and kidneys of mouse X and immunodeficient recipients R_2, R_3, and R_4. 37 out of 38 sequences were derived from a VHJ558 (AF303848/BC018315 in BALB/c), D-SP2.2 (J00431), JH4 (V00770) rearrangement with identical VDJ junctions. The J558 sequence has not been confirmed as a germline sequence at the genomic level, but the identical sequence from cDNA has been identified by numerous independent researchers, indicating that it does represent a germline gene (3, 4). The sequences are given in this figure and an overview is given in Fig. 6. Unmutated-30 indicates 30 identical unmutated sequences derived from mice and organs as indicated in Fig. 6 B (left panel, unmutated). The rest of the sequences are given as "mouse-organ-isotype," where X is the originator mouse; R_2–R_4 are recipients; S (spleen), L (liver), and K (kidney) are the organs; and μ, γ3, γ1, and γ2a are the isotypes of the H chain. For X-K-μ-2, 2 indicates two identical sequences. An overview of these sequences is found in Fig. 6 B(left panel, mutated). 1 out of 38 sequences, detected in the kidney of mouse X with γ1 isotype (X-K-γ1), was derived from a different V_H, had different VDJ junctions, and was probably derived from a normal B cell (not depicted). Dots represent identity with the representative germline sequences and dashes represent gaps for optimal alignment. Sequences X-S-γ1-1 and R4-S-μ-1 have a nucleotide insertion in FR3 that cause a frame shift that results in stop codons in FR3.

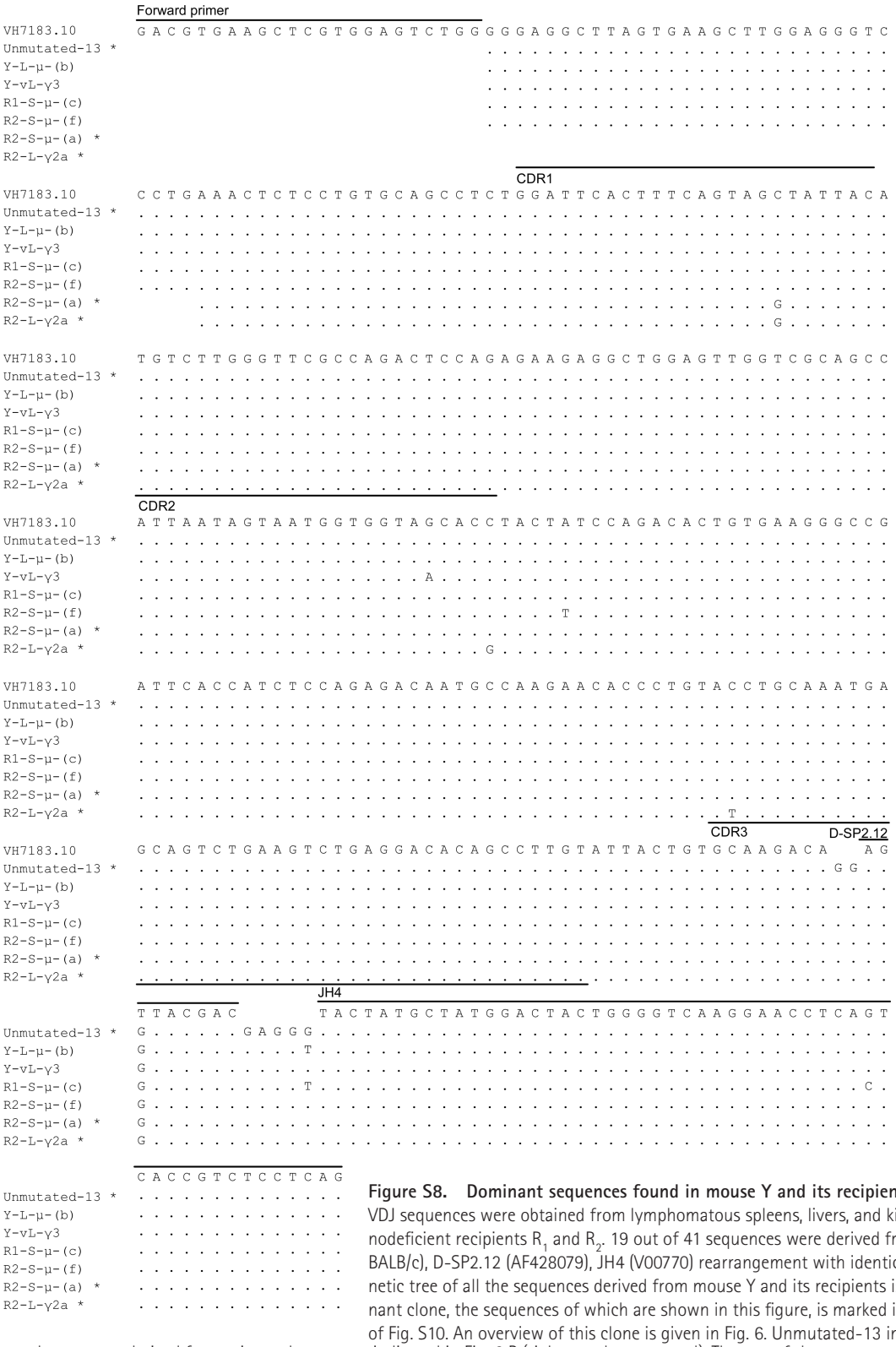

Figure S8. Dominant sequences found in mouse Y and its recipients. Altogether, 41 rearranged VDJ sequences were obtained from lymphomatous spleens, livers, and kidneys of mouse Y and immunodeficient recipients R_1 and R_2. 19 out of 41 sequences were derived from a VH7183.10 (AF290962, in BALB/c), D-SP2.12 (AF428079), JH4 (V00770) rearrangement with identical VDJ junctions. A phylogenetic tree of all the sequences derived from mouse Y and its recipients is given in Fig. S10. The dominant clone, the sequences of which are shown in this figure, is marked in red in the phylogenetic tree of Fig. S10. An overview of this clone is given in Fig. 6. Unmutated-13 indicates 13 identical unmutated sequences derived from mice and organs as indicated in Fig. 6 B (right panel, unmutated). The rest of the sequences are given as "mouse-organ-isotype," where Y is the originator mouse; R_1 and R_2 are recipients; S (spleen) and L (liver) are the organs; and μ, γ3, and γ2a are the isotypes of the H chain. Non-identical sequences of the same mouse-organ-isotype are distinguished by lowercase letters in parentheses. An overview of these sequences is found in Fig. 6 B (right panel, mutated). Dots represent identity with the representative germline sequences. Stars represent sequences (including 3 out of the 13 unmutated) where the 3′IgE C-region primer has been chosen from the primer mixture as 5′ primer in antisense 5′-3′ direction aligning to the V_H.

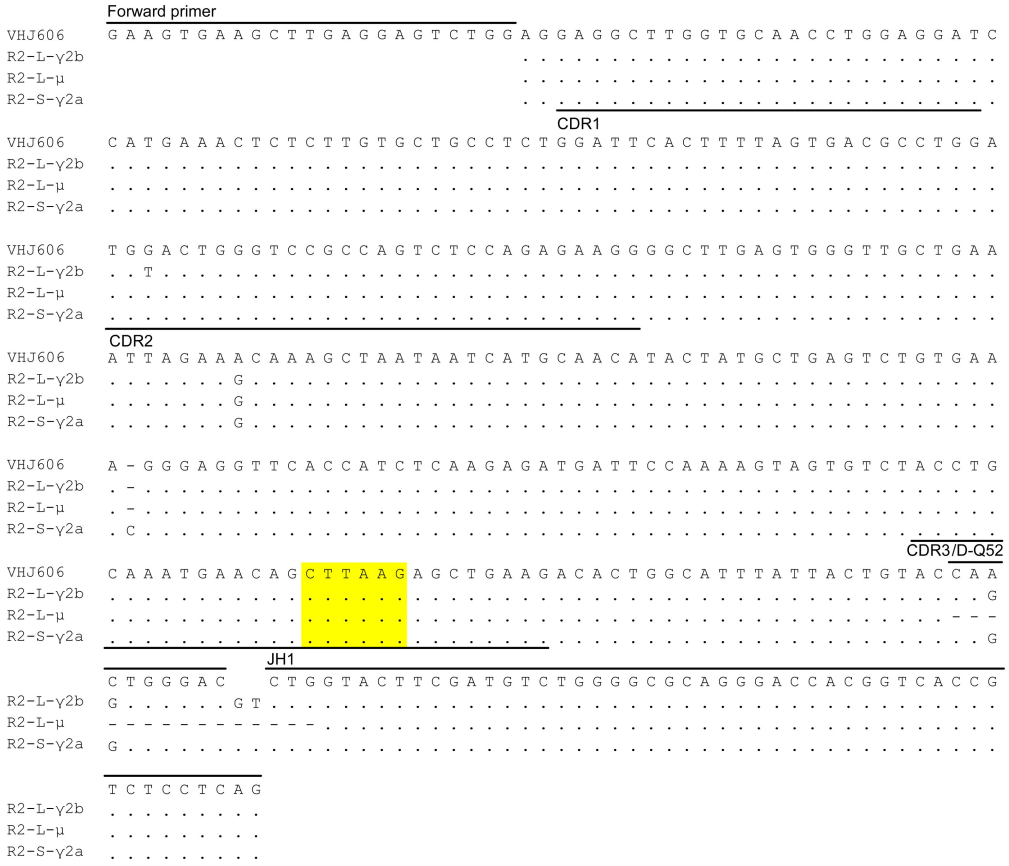

Figure S9. Minor sequences found in mouse Y recipients. Altogether, 41 rearranged VDJ sequences were obtained from lymphomatous spleens, livers, and kidneys of mouse Y and immunodeficient recipients R_1 and R_2. In addition to the dominant sequence described in Fig. S8, 3 out of 41 sequences, all detected in R_2, were derived from a VHJ606 (ME3, M59921/M59922), D-Q52 (J00440), JH1 (V00762) rearrangement that had identical VDJ junctions. The ME3 sequence has been confirmed as a germline gene at the genomic level (5). Note that R2-L-μ had a deletion of the DJ junctional sequence. The sequence of R2-S-γ2a had a nucleotide insertion in FR3, causing a frame shift and stop codon in FR3. A phylogenetic tree of all the sequences from mouse Y and recipients is given in Fig. S10. The minor clone emerging in R_2, the sequence of which is shown in this figure, is marked with blue in the phylogenetic tree. The names of the sequences are given as "mouse-organ-isotype," where R_2 is the second recipient; S (spleen) and L (liver) are the organs; and μ, γ2a, and γ2b are the isotypes of the H chain. Dots represent identity with the representative germline sequences and dashes represent gaps for optimal alignment. An EcoRI restriction site in FR3 is in yellow. This site probably explains the smallest monoclonal VDJ rearrangement seen in EcoRI-digested R_1 lymphoma DNA probed with a downstream J_H probe. See Fig. S11 for J_H Southern.

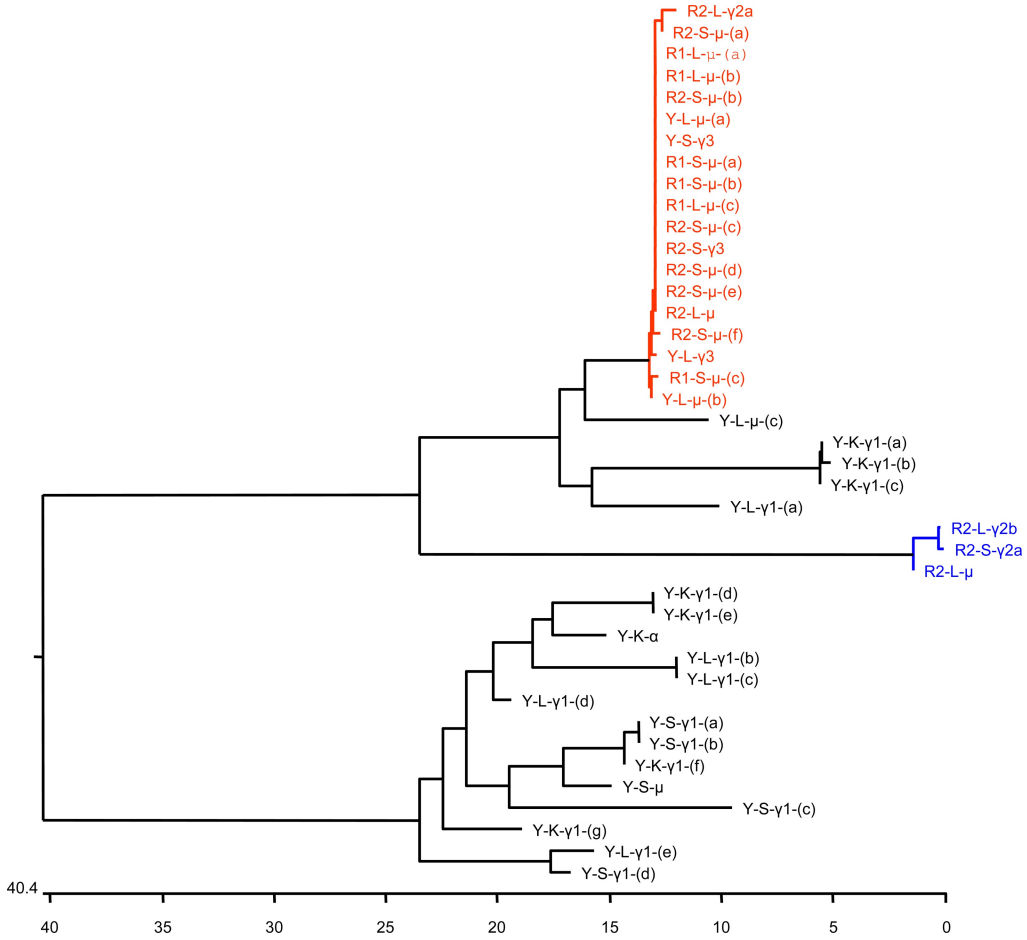

Figure S10. Interclonal relationship of clones obtained from mouse Y and its recipients. Phylogenetic tree showing the relationship between the sequences obtained from lymphomatous spleens, livers, and kidneys of mouse Y and immunodeficient recipients R_1 and R_2. In lymphoma mouse Y, a monoclonal population (≈20%) was admixed with a polyclonal V_H repertoire. After transfer, the monoclonal population dominated in the R_1 and R_2 mouse. The dominant clone is shown in red and detailed in Fig. 6, and sequences are given in Fig. S8. After the second transfer (R_2) another minor clone was detected in addition (blue; detailed in Fig. S9), resulting in a biclonal picture in R_2. (The minor clone must also have been presented in mouse Y and R_1 but was not detected, sequencing of more colonies from Y and R_1 should probably have revealed it. The clone is probably represented by the lower band in the J_H Southern of the YR_1 lymphoma [see Fig. S11].). The length of each pair of branches represents the distance between sequence pairs. The units at the bottom of the tree indicate the number of substitutions. The names of the sequences are given as "mouse-organ-isotype," where Y is the originator mouse;, R_1 and R_2 are recipients; S (spleen), L (liver), and K (kidney) are the organs; and μ, γ3, γ1, γ2a, and γ2b are the H chain isotypes. Non-identical sequences of the same mouse-organ-isotype are distinguished by letters in parentheses.

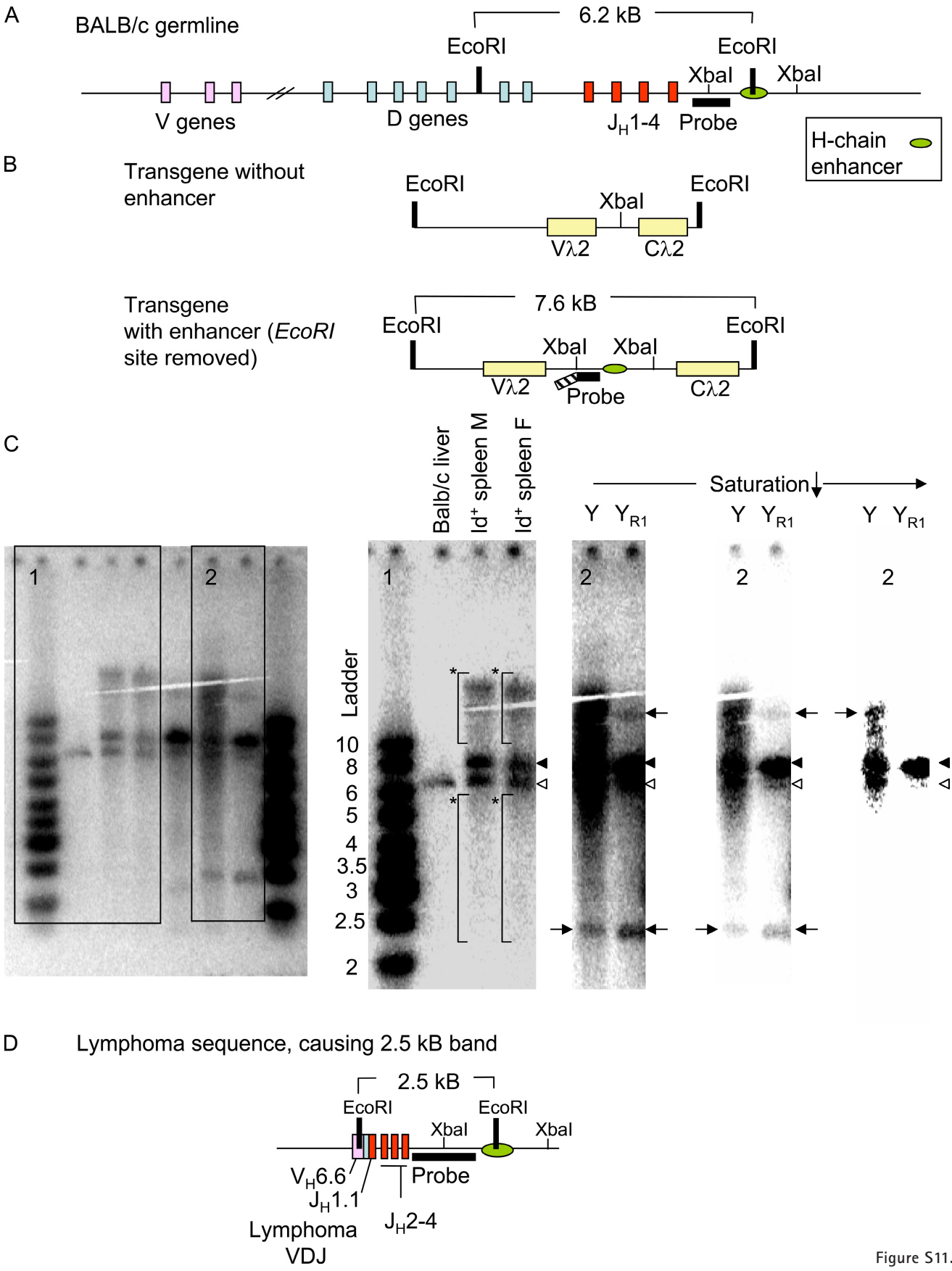
A
BALB/c germline
6.2 kB
EcoRI
EcoRI
XbaI
XbaI
V genes
D genes
J_H1-4
Probe
H-chain enhancer
B
Transgene without enhancer
EcoRI
XbaI
EcoRI
Vλ2
Cλ2
Transgene with enhancer (*EcoRI* site removed)
7.6 kB
EcoRI
EcoRI
XbaI
XbaI
Vλ2
Probe
Cλ2
C
Balb/c liver
Id+ spleen M
Id+ spleen F
Saturation
Y
Y_{R1}
Ladder
10
8
6
5
4
3.5
3
2.5
2
1
2
D
Lymphoma sequence, causing 2.5 kB band
2.5 kB
EcoRI
EcoRI
XbaI
XbaI
V_H6.6
J_H1.1
Probe
J_H2-4
Lymphoma VDJ

Figure S11.

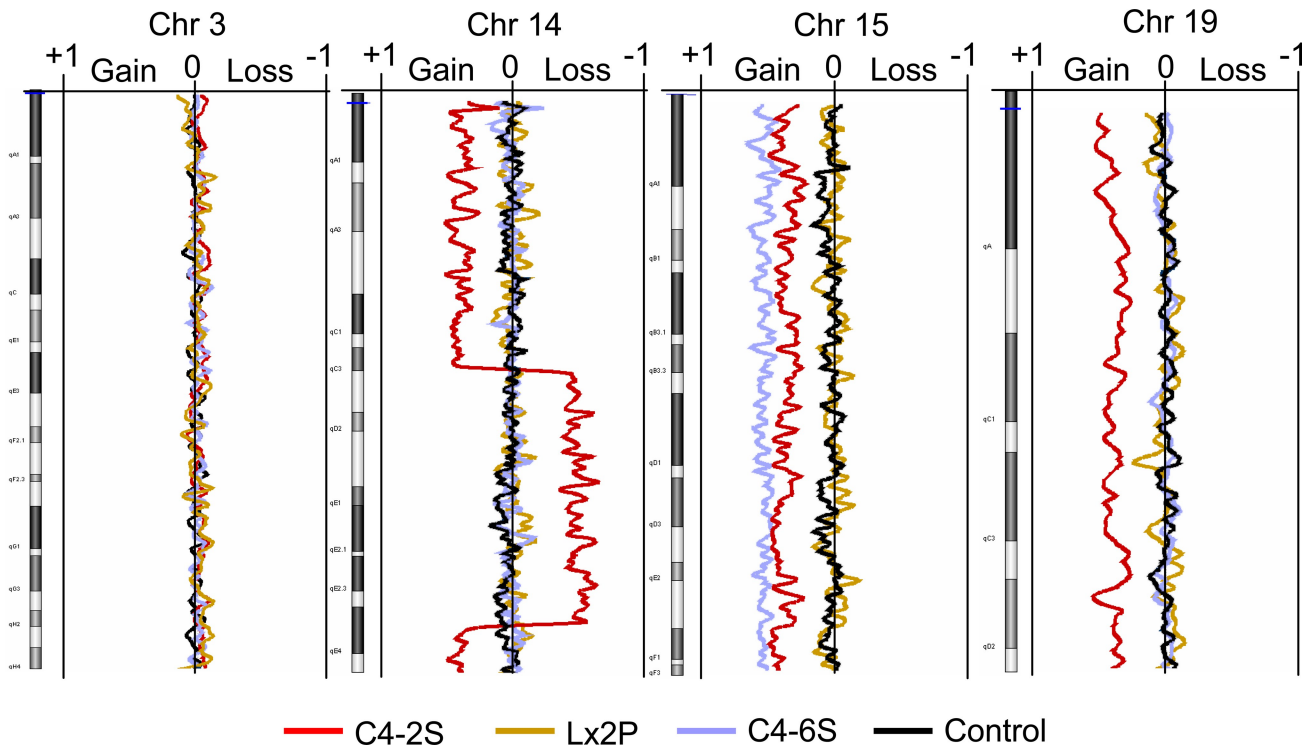

Figure S12. Genomic DNA aberrations are prevalent in the lymphomas. Some examples are shown. Lymphoma spleen DNA and Id^+ control DNA (from a male mouse) were fluorescently labeled and competitively hybridized to oligonucleotide genomic microarrays. As examples, chromosomal gains and losses on Chromosome 3, 14, 15, and 19 are shown for three independent lymphoma lines (C4-2S, C4-6S, and Lx2P), as well as a control female/male Id^+ mouse hybridization. As a control, DNA from one healthy female Id^+ mouse competed with that of the Id^+ male. Lines deviating from the central zero indicate gains (left) or losses (right). The +1 (gain) and −1 (loss) lines (in Log2) represent two extra copies or one missing copy, respectively. Data for all autosomes of six lymphoma lines are shown in Fig. S13.

Figure S11. Southern analysis of EcoRI-digested Y lymphoma DNA with downstream J_H probe. A Southern was designed to detect VDJ rearrangements, as well as the Id^+ transgene (engineered with an H-chain enhancer). (A) Genomic map of BALB/c DJC region (For further details see: http://imgt.cines.fr/textes/IMGTrepertoire/LocusGenes/locus/mouse/IGH/Mu_IGHmap.html). A 0.8-kb EcoRI fragment containing part of JH-Cμ intron was used as probe (6). The probe (black bar) binds immediately downstream of the J_H4 and upstream of the H-chain enhancer. This probe can also hybridize to the Id^+ $\lambda2^{315}$ transgene construct. (B) Transgenes used for construction of the Id^+ mouse (7). (top) EcoRI fragment containing the λ2 gene of MOPC315 (8). (bottom) The Mouse Ig H-chain enhancer (9, 10) of the Sp6 H-chain gene was introduced as a 1-κB XbaI fragment into the XbaI site. The EcoRI site in the enhancer was removed by in vitro mutagenesis. Note that the probe indicated in A hybridizes to parts of the XbaI fragment as indicated (black section of probe bar). Equal numbers of the λ2 gene with and without the H-chain enhancer were injected into pronuclei of fertilized (CBA/BrAxC57/Bl/LiA) eggs. The selected founder contained ?15 copies of each construct cointegrated on the same chromosome (7). (C) Southern blot of the indicated EcoRI digested hybridized with the probe as indicated in A and B. (left) The original scan is shown. The two indicated areas (1 and 2) are presented on the right. (area 1) Genomic BALB/c liver DNA gives rise to the germline IgH band (6.2 kB, open arrowhead). The Id^+ spleens have an additional band (closed arrowhead), corresponding to the $\lambda2^{315}$ transgene with the inserted XbaI fragment (B, bottom). In addition, diffuse signals (asterisk) correspond to oligo/polyclonal B cell VDJ or DJ rearrangements; these are indeed not found in the liver. (area 2) Three different decremental levels of saturation are shown for spleen DNA from the mouse that developed the lymphoma Y and its first $RAG2^{-/-}$ recipient (Y_{R1}). The Y lymphoma has been extensively characterized by sequencing (Fig. 6 and Fig. S8–S10): mouse Y had a polyclonal set of sequences, only two of which were found in lymphomatous mice after sequential transfers to recipients. Consistent with these data, the J_H Southern blot of the spleen of mouse Y shows clear polyclonality. However, in the lymphomatous Y_{R1} $RAG2^{-/-}$ recipient, the polyclonality is clearly reduced and two clonal VDJ rearrangement bands are seen (arrows). These bands are also seen in the Y lymphoma originator mouse. Thus, the Southern analysis was consistent with the sequencing results, describing a biclonal lymphoma emerging from a polyclonal background. (D) The low molecular weight (≈2.5 kB) of the lowest band in Y_{R1} (and Y) suggested that an EcoRI site might be present in the V region of the monoclonal VDJ rearrangement resulting in this band. This was indeed found to be the case because an EcoRI site was found in FR3 in one of the two sets of independent monoclonal sequences in the biclonal lymphoma (Figs. S9 and S10). The distance between the two EcoRI sites in the rearranged VDJ sequence was calculated to be 2.5 kB, thus strongly linking this clone to the ≈2.5-kB band in the J_H Southern (Fig. S9, γ2a, γ2b, and μ clones). Note that this band is detected in the Y lymphoma originator mouse, but was detected by sequencing only after transfer.

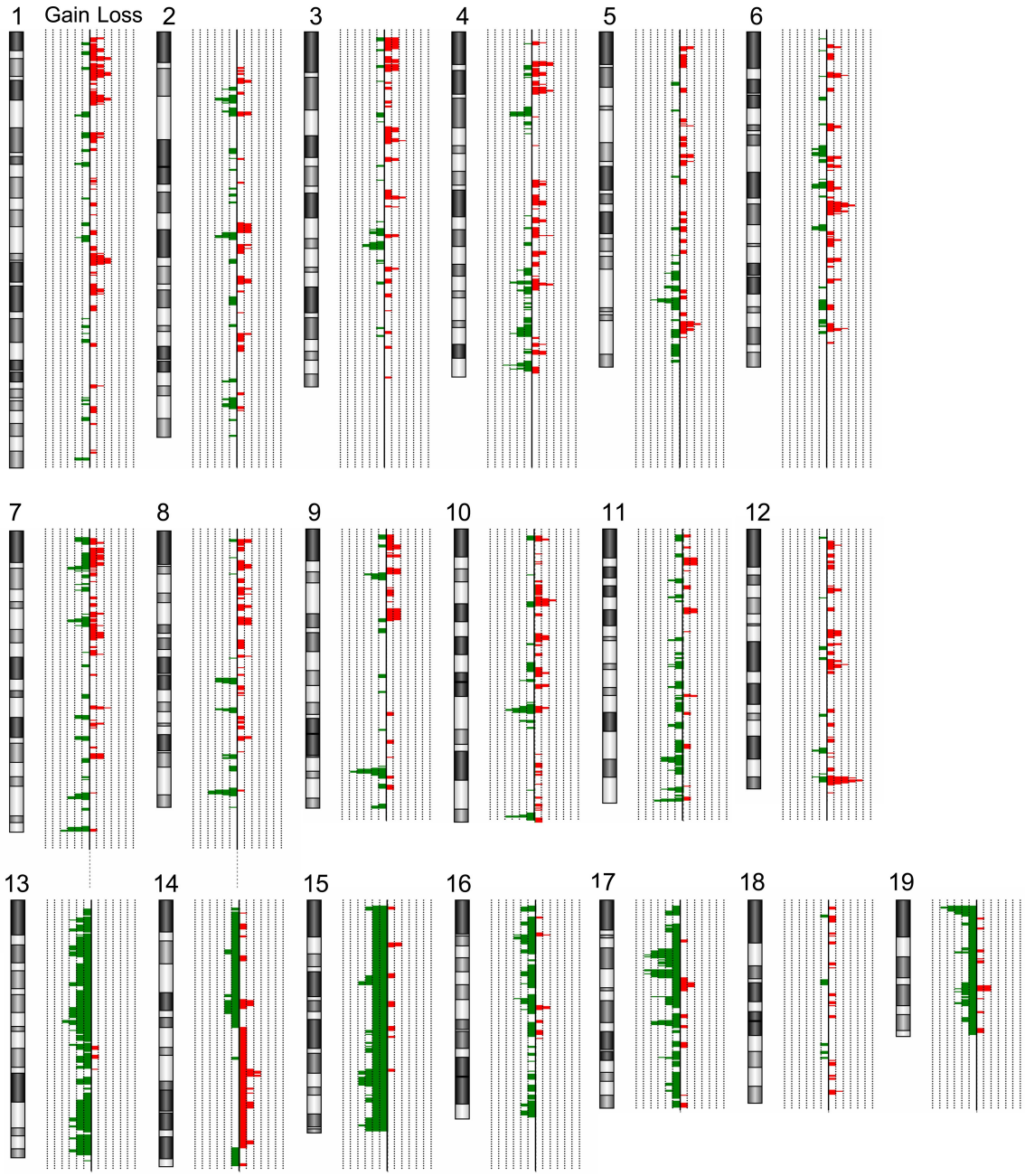

Figure S13. Frequency plot of chromosomal aberrations in all autosomes of six independent lymphomas. The figure shows a frequency plot of chromosomal gains or losses in the six independent lymphoma lines. Amplifications (green) and deletions (red) are shown for each autosomal chromosome. The height of the columns indicates the number of lymphomas (out of six) with gains or losses in the particular chromosomal area. Overall, the data suggest recurrent genetic changes. Gains and losses were scored using a z score algorithm (threshold two), with a minimum of three consecutive oligos and a 1-Mb moving window size. A male/female hybridization, as well as whole chromosomes gains or losses, were used to optimize the algorithm threshold.

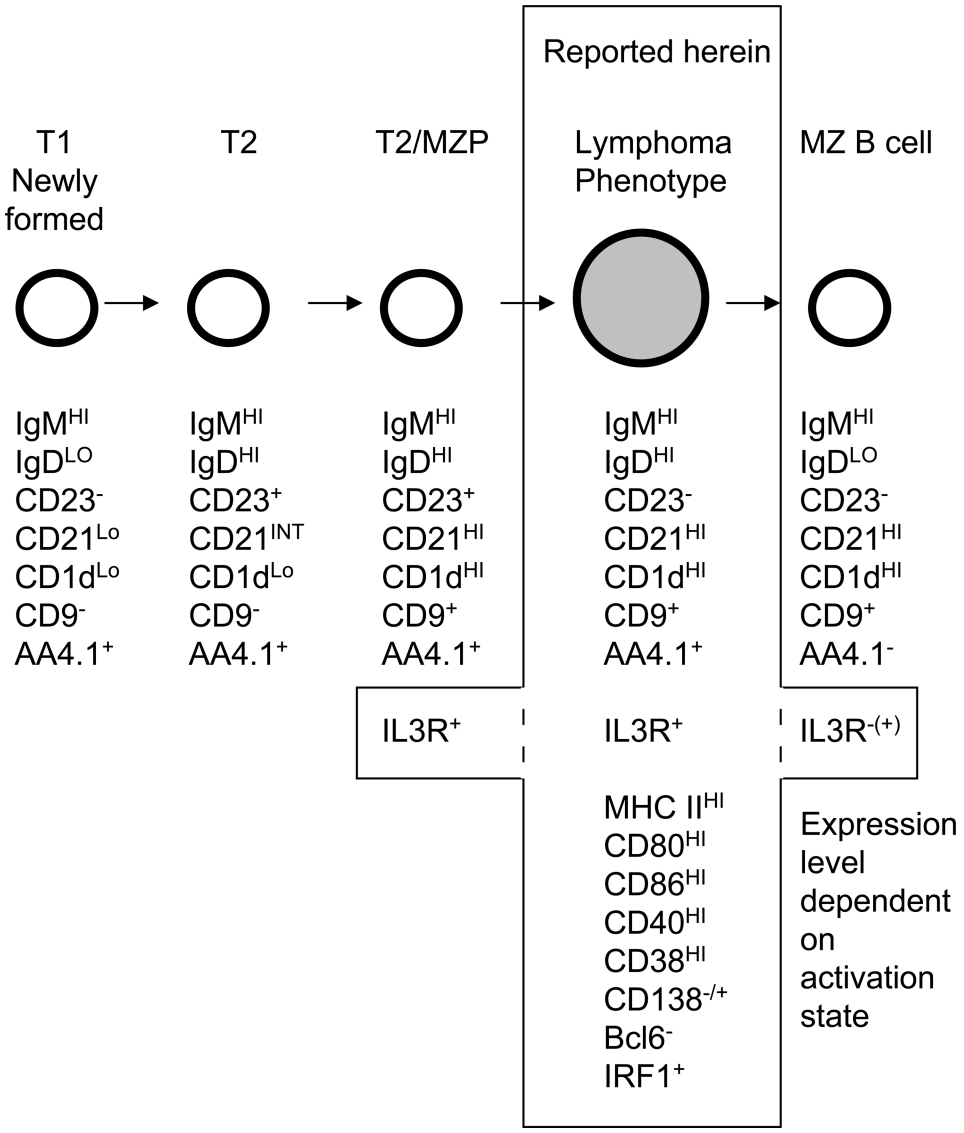

Figure S14. Summary of lymphoma markers. Schematic summary of lymphoma phenotype compared with conventional stages of marginal zone development as suggested in Pillai et al. (1). Information is also included on IL-3R expression (see Fig. S4).